

# Performance Evaluation of Photovoltaic String with Compound Parabolic Concentrator

Haider Ali and P. Gandhidasan

**Abstract**—Photovoltaic (PV) system is used to directly converting the solar energy into the electrical energy. Compound Parabolic Concentrator (CPC) is a non-imaging concentrator which is considered in this study for reducing the cost of electrical energy. Two configurations are numerically studied namely one with simple typical flat PV string and the other PV string with CPC. The truncated CPC with concentration ratio of 2.3 and an acceptance angle of  $41.75^\circ$  is considered in the analysis of PV string with CPC (PV-CPC). Transient System Simulation Software (TRNSYS) is used for the evaluation of PV cell performance with and without CPC. The mathematical model for PV and PV-CPC is developed for the performance estimation of thermal and electrical characteristic of the system. Engineering Equation Solver (EES) code is written to solve the mathematical model and is linked with TRNSYS for simulation. The simulation is carried out for the average day of the months of June and December for Riyadh city. Results indicated that the use of the CPC increases the absorbed energy and electrical power output of PV system. The electrical power of PV string increases almost 35% when CPC is used with PV compared to simple typical flat PV string.

**Index Term**—Compound parabolic concentrator, TRNSYS, photovoltaic string, performance analysis.

## I. INTRODUCTION

Solar energy is considered as renewable and environment friendly energy source for meeting the world energy demands. Solar energy utilization can be classified into two categories: one is thermal system that converts solar energy into thermal energy, and the other is photovoltaic (PV) system that converts solar energy directly into electrical energy [1].

Since the PV technology improves and maximizes the photoelectrical conversion rates, it has been extensively employed in the recent years. Due to the high initial capital cost of PV systems, their wide-ranging applications are restricted. The cost can be reduced either by increasing the efficiency of the solar cell or using concentration photovoltaic (CPV). A cost-effective and improved CPV system is obtained by producing the same amount of power by using less number of cells compared to conventional number of cells. It is reported that a low concentration photovoltaic system (LCPV) can reduce the cost up to 40% compared to a simple flat PV system [2], [3]. Due to their potentials of non-tracking, high liability and low cost, a considerable amount of research has been done for the development of various types LCPV applications [4]. Many efforts have been made in the recent years by using CPC to reduce the use of

expensive solar cells and hence lower the cost of PV power output [5]–[8]. Concentration ratios in the range of 2–7 can be obtained with simple CPC which needs only the seasonal tilt adjustments rather than tracking the sun. To determine the yearly optimal tilt-angle of aperture to maximize the annual collectible radiation on the absorber of CPC and finding the optimal acceptance half-angle, a mathematical model was presented by Tang *et al.* [9].

Nilsson *et al.* [6] use MINSUN simulation program for the estimation of annual thermal and electrical output from PV-CPC thermal hybrid system. Effects of optical properties on the thermal and electrical efficiencies of PV cells were also studied by researchers [10], [11]. Thermal and electrical performances of PV-CPC system are also studied numerically [1], [12], [13] as well as experimentally [14]. Kalogirou [15] used Transient System Simulation (TRNSYS) software for modeling and simulation of a simple PV system. TRNSYS is very powerful tool which is developed for the analysis of different solar energy applications as well as for simulation of a variety of thermal processes but PV-CPC system is not simulated using TRNSYS. In the present study performance of PV string is evaluated using TRNSYS with CPC. The performance characteristics of photovoltaic string are studied for the climatic condition of Riyadh, Saudi Arabia and two cases are analyzed: i) simple flat PV string and ii) PV string with CPC. Effects of CPC on the absorbed radiation and the power output of the PV string are simulated using the TRNSYS software. Since, the PV-CPC component with flat receiver is not available in TRNSYS, the codes are developed using the Engineering Equation Solver (EES) software to solve the mathematical models for thermal and electrical characteristics. The EES code is then coupled with TRNSYS software to run simulations.

## II. SYSTEM MODEL

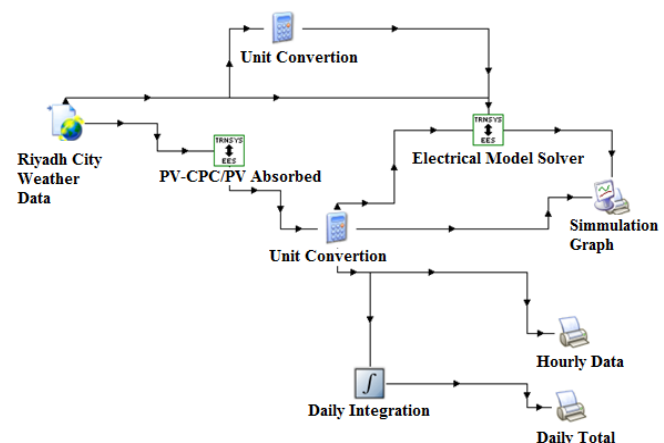


Fig. 1. Flow diagram for various components connection in TRNSYS.

Manuscript received March 25, 2014; revised June 26, 2014.

The authors are with the Mechanical Engineering Department of King Fahd University of Petroleum & Minerals, Dhahran 31261, Saudi Arabia (tel: 966-3-860-2096; e-mail: haiali@kfupm.edu.sa, pgandhi@kfupm.edu.sa).

TRNSYS consists of many subroutines, in which mathematical models are given in terms of ordinary differential or algebraic equation. First step in TRNSYS is to identifying the all system components and in the second step, all components connected according to the information flow diagram of the system. Two codes are developed in EES software: one to solve the mathematical model for absorbed energy and the other to solve the mathematical model of electrical characteristics for PV and PV-CPC. These codes are coupled with the TRNSYS using the EES calling component option. Fig. 1 shows the flow diagram that connects the various components in the TRNSYS software.

### III. MATHEMATICAL MODELING

A standard CPC is modeled for the PV cell width of 134 mm and with 38% truncation with an half acceptance angle is  $41.75^\circ$ . The geometrical concentration for truncated CPC is 2.3X and aluminum is considered as the material for the reflecting surface of CPC.

#### A. Optical Model

The amount of solar radiation incident on the tilted surface is estimated by using isotropic diffuse model. CPC has the advantage that it does not required continuous tracking. But to get the maximum output from the collector, CPC should be properly oriented along east-west axis and tilted towards due south with appropriate slope and seasonal adjustment. In order to estimate the total amount of absorbed radiation by the PV-CPC system, the contribution of beam, diffuse and ground reflected and beam components are need to be determined.

$$S_{CPC} = G_{b,CPC} \tau_{CPC,b} (\tau\alpha)_b + G_{d,CPC} \tau_{CPC,d} (\tau\alpha)_d + G_{g,CPC} \tau_{CPC,g} (\tau\alpha)_g \quad (1)$$

The transmittance-absorptance product of solar cell is calculated for beam, diffuse and ground reflected radiation.

$$\tau_{cpc} = \rho^{n_i} \quad (2)$$

where  $\tau_{cpc}$  is the transmittance of the CPC, it accounts for the specular reflectance of the concentrator and the average number of reflection.

Beam, diffuse and ground reflected radiation are calculated using the following formulae [16]:

$$G_{b,CPC} = F G_{bn} \cos \theta \quad (3)$$

where  $F$  is the control function, which is 1 if  $(\beta - \theta_c) \leq \tan^{-1}(\tan \theta_z \cos \gamma_s) \leq (\beta + \theta_c)$  otherwise it is zero.

$$G_{d,CPC} = \begin{cases} \frac{G_d}{C} & \text{if } (\beta + \theta_c) < 90^\circ \\ \frac{G_d}{2\left(\frac{1}{C} + \cos \beta\right)} & \text{if } (\beta + \theta_c) > 90^\circ \end{cases} \quad (4)$$

$$G_{g,CPC} = \begin{cases} 0 & \text{if } (\beta + \theta_c) < 90^\circ \\ \frac{G_g}{2\left(\frac{1}{C} - \cos \beta\right)} & \text{if } (\beta + \theta_c) > 90^\circ \end{cases} \quad (5)$$

where  $G_g = G \rho_g$ .

To calculate the absorbed radiation by PV the modified isotropic diffuse model is given by [16].

$$\frac{S_{PV}}{S_{ref}} = M \left( \frac{G_b}{G_{ref}} R_b K_{\tau\alpha,b} + \frac{G_b}{G_{ref}} K_{\tau\alpha,d} \left( \frac{1 + \cos \beta}{2} \right) + \rho_g \frac{G}{G_{ref}} K_{\tau\alpha,g} \left( \frac{1 - \cos \beta}{2} \right) \right) \quad (6)$$

where

$$S_{ref} = M_{ref} G_{ref} (\tau\alpha)_n \quad (7)$$

And

$$R_b = \frac{\cos \theta}{\cos \theta_z} \quad (8)$$

#### B. Thermal Model

Absorbed radiation estimated from the optical model is employed to evaluate the thermal model for the temperature distribution within the layers of the PV-CPC system.

Following assumptions are made while modeling the thermal network for the PV-CPC system:

- 1) Energy transfer in the problem is 1-D and steady state of energy transfer is considered.
- 2) The capacity of the glass cover and solar cell is neglected.
- 3) Temperature variation along the thickness and width is negligible.
- 4) There is no dust and dirt effect on the collector.

Based on the above assumptions the energy balance equations can be written on the different components of the PV-CPC system.

Energy balance on PV cell is given by,

$$S_{cpc} = U_t (T_c - T_a) + U_{chs} (T_c - T_{bs}) \quad (9)$$

The radiation heat transfer coefficient from glass cover to the ambient is given by [16],

$$h_{r,ca} = \varepsilon_g \sigma (T_g^2 + T_a^2) (T_g + T_a) \quad (10)$$

The wind-related heat transfer coefficient  $h_w$  is given by McAdams [17].

$$h_w = 5.7 + 3.8 V_w \quad (11)$$

Overall heat transfer coefficient is calculated solving the thermal network shown in Fig. 2.

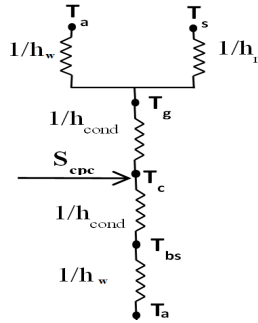


Fig. 2. Thermal network.

### C. Electrical Model

The electrical characteristic is calculated using the five parameter model. In this model the PV cell is represented by an equivalent circuit as shown in Fig. 3. Current-Voltage ( $I$ - $V$ ) characteristic of this model is defined by [16]:

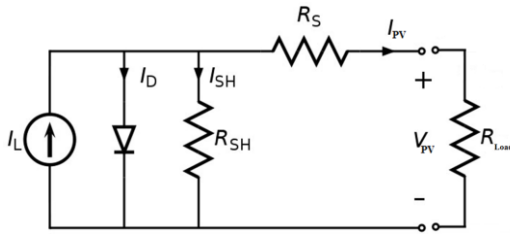


Fig. 3. Equivalent circuit of a PV cell.

$$I = I_L - I_0 \left[ \exp \left( \frac{(V + IR_S)}{a} \right) - 1 \right] - \frac{V + IR_S}{R_{SH}} \quad (12)$$

The following five conditions in Table I are used to estimate the five parameters:

TABLE I: FIVE CONDITIONS AND FIVE PARAMETERS

At short circuit	$[dI/dV]_{sc} = -1/R_{sh,ref}$
At open circuit voltage	$V = V_{oc,ref}, I = 0$
At short circuit current	$V = 0, I = I_{sc,ref}$
At the maximum power point	$V = V_{mp,ref}, I = I_{mp,ref}$
At the maximum power point	$[dI/dV]_{mp} = 0$

Using the above conditions into (13) the following equations are obtained:

$$I_{sc,ref} = I_{L,ref} - I_{0,ref} \left[ \exp \left( \frac{V_{oc,ref}}{a_{ref}} - 1 \right) \right] - \frac{I_{sc,ref} R_{s,ref}}{R_{sh,ref}} \quad (13)$$

$$I_{L,ref} = I_{0,ref} \left[ \exp \left( \frac{V_{oc,ref}}{a_{ref}} - 1 \right) \right] + V_{oc,ref} / R_{sh,ref} \quad (14)$$

$$I_{mp,ref} = I_{L,ref} - I_{0,ref} \left[ \exp \left( \frac{V_{mp,ref} + I_{mp,ref} R_{s,ref}}{a_{ref}} \right) - 1 \right] - \frac{V_{mp,ref} + I_{mp,ref} R_{s,ref}}{R_{sh,ref}} \quad (15)$$

$$\frac{I_{mp,ref}}{V_{mp,ref}} = \frac{\frac{I_{0,ref}}{a_{ref}} \left[ \exp \left( \frac{V_{mp,ref} + I_{mp,ref} R_{s,ref}}{a_{ref}} \right) \right] + \frac{1}{R_{sh,ref}}}{1 + \frac{I_{0,ref} R_{s,ref}}{a_{ref}} \left[ \exp \left( \frac{V_{mp,ref} + I_{mp,ref} R_{s,ref}}{a_{ref}} \right) \right] + \frac{R_{s,ref}}{R_{sh,ref}}} \quad (16)$$

In this present study EES is used to evaluate these five parameters at reference conditions  $T_{cell,ref} = 25^\circ\text{C}$ ,  $G_{ref} = 1000 \text{ W/m}^2$ . The  $I_{mp}$ ,  $V_{mp}$  and  $P_{mp}$  can be obtained at any operating conditions.

$$P_{mp,string} = I_{mp} V_{mp,string} \quad (17)$$

Electrical efficiency can now be calculated based on these parameters as the amount of electrical output to the amount of input solar energy incident on the PV string.

$$\eta_{el,mp} = \frac{I_{mp} V_{mp}}{CA_c G_T} \quad (18)$$

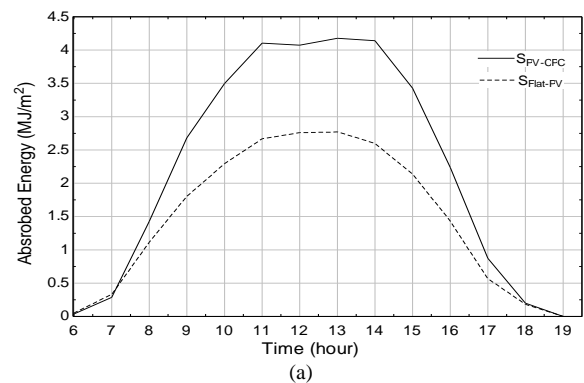
## IV. RESULTS AND DISCUSSION

Simulation is performed for the average day of two months of the year namely June and December in TRNSYS 16.

In initial simulation results the shading effects is observed. To remove the shading effect some adjustment in the slope is done. For June, slope =  $\phi - 17.5^\circ$  and for December,  $\phi + 17.5^\circ$  is used in simulation.

Fig. 4 shows the simulation results of absorbed radiation for average day of the months. It is observed that absorbed energy is increased with PV-CPC system. Fig. 4(a) shows the results for the average day of month of June. In this month the amount of absorbed energy increase from  $2.8 \text{ MJ/m}^2$  for flat PV string to  $4.2 \text{ MJ/m}^2$  for PV-CPC string. The result of average day of the month of December is shown in Fig. 4(b). The maximum absorbed energy for flat PV string is  $2.87 \text{ MJ/m}^2$  and for PV-CPC string its value is  $4.70 \text{ MJ/m}^2$ .

Electrical power output for average day of months is shown in Fig. 5. It is evident from Fig. 5 that the use of CPC enhances the performance of PV string. Fig. 5(a) shows the power out for the average day of month of June. The maximum power output is increased from  $13.3 \text{ W}$  to  $17.2 \text{ W}$ . The power output result for average day of month of December is shown in Fig. 5(b). The maximum power output increases from  $15.2 \text{ W}$  to  $19.7 \text{ W}$ .



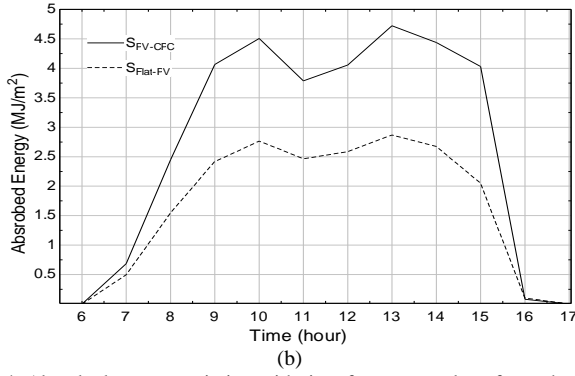


Fig. 4. Absorbed energy variation with time for average day of month of (a) June and (b) December.

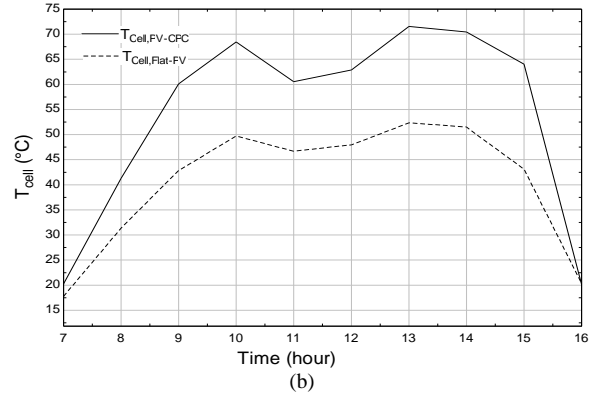


Fig. 6. Cell temperature variation with time for average day of month of (a) June and (b) December.

Higher temperature resulted in lower efficiencies of PV-CPC system.

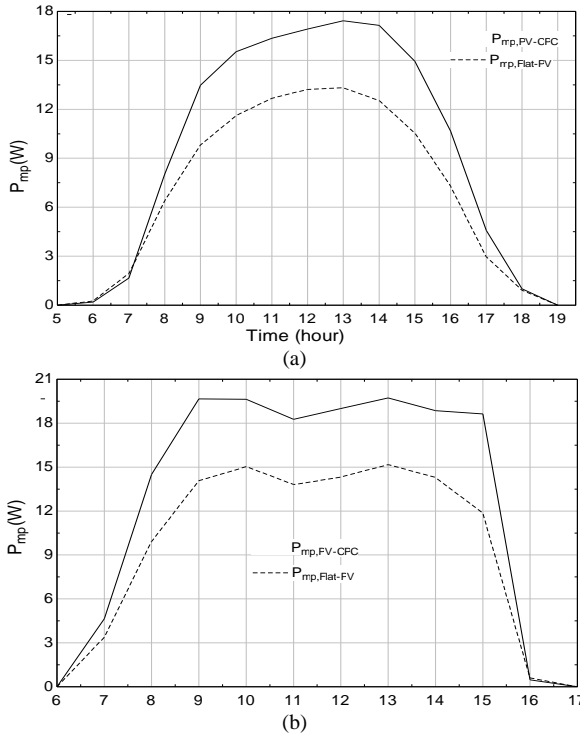


Fig. 5. Maximum power output variation with time for average day of month of (a) June and (b) December.

Fig. 6 shows the cell temperature for the month of June and December. The cell temperature of PV-CPC string is higher compared to the flat PV string. Fig. 7 shows the efficiency for the month of June and December. Although the power output from PV-CPC string is higher compared to the flat PV string, but efficiency of PV-CPC is lower in comparison to flat PV string. This is because the input incident radiation is more on PV-CPC system, which resulted in higher output of system and higher temperature.

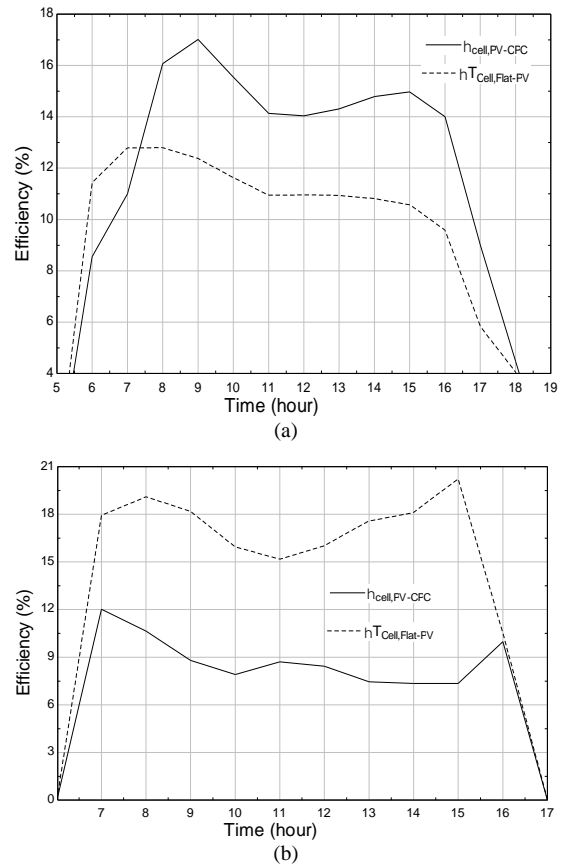


Fig. 7. Efficiency variation with time for average day of month of (a) June and (b) December.

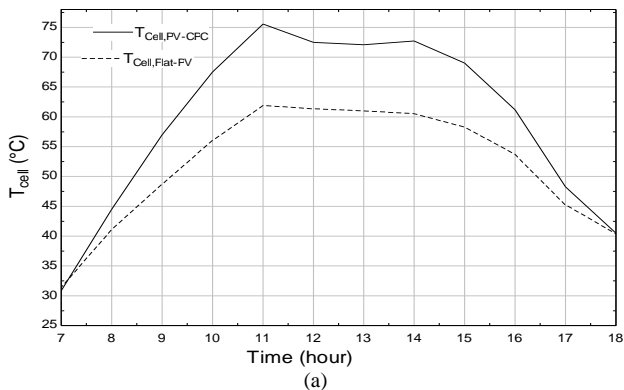


Fig. 8 shows the total of absorbed radiation. The results clearly indicate that energy increased with use of PV-CPC configuration. The absorbed energy is increased by 50.5% with PV-CPC string compared to flat PV string for month of June while for the month of December the use of CPC result in 64.8% increase in absorbed energy.

Fig. 9 shows the total power output for the average day of the months. Fig. 9 shows that use of CPC also improves the power output of the PV string. For the average day of the month of June the electrical power output for the day is increased by 33.1% with the use of CPC. The electrical power the day for PV-CPC is increased by 36.4% compared to flat PV string for the month of December.

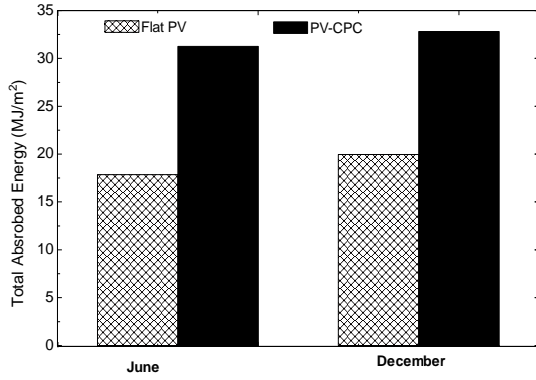


Fig. 8. Total absorbed energy for the average day of the months Circuit

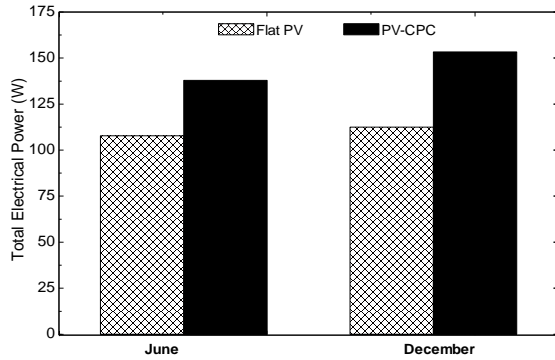


Fig. 9. Total electrical power for the average day of the months.

## V. CONCLUSION

In this the performance of the flat PV and PV-CPC system is investigated for the Riyadh city, KSA. The TRNSYS is used for the simulations in combination with EES to solve mathematical models. Some seasonal adjustment of slope PV string is performed for the removal of shading effect. It is found that the performance of the PV string is enhanced with the use CPC. The PV-CPC string gives higher values of the absorbed energy and electrical power output as compared to the flat PV string. The increase in absorbed energy by PV-CPC string also results in the increment in cell temperature, which results in dropping the electrical efficiency of PV-CPC string. The performance of PV-CPC system can be enhanced by cooling the PV string.

## NOMENCLATURE

$a$ : ideality factor  
 $A_c$ : area of the PV module ( $m^2$ )  
 $C$ : geometrical concentration  
 $G_{b,CPC}$ : beam component of the radiation ( $MJ/m^2$ )  
 $G_{ref}$ : solar radiation at a reference condition at the normal incidence angle ( $MJ/m^2$ )  
 $G_T$ : amount of incident radiation ( $MJ/m^2$ )  
 $h_w$ : heat transfer coefficient ( $W/K.m^2$ )  
 $I$ : current at load (A)  
 $I_L$ : light current (A)  
 $I_{mp}$ : maximum power point current (A)  
 $I_{sc}$ : short circuit current (A)  
 $I_o$ : diode saturation current (A)  
 $M$ : air mass modifier  
 $M_{ref}$ : air mass modifier at reference condition (=1)  
 $n_i$ : number of reflection

$R_b$ : ratio of beam radiation  
 $R_s$ : series resistance ( $\Omega$ )  
 $R_{sh}$ : shunt resistance ( $\Omega$ )  
 $S$ : absorbed radiation ( $MJ/m^2$ )  
 $S_{CPC}$ : amount of energy absorbed by PV-CPC ( $MJ/m^2$ )  
 $T_a$ : ambient temperature ( $^{\circ}C$ )  
 $T_g$ : glass cover temperature ( $^{\circ}C$ )  
 $T_{bs}$ : back surface temperature ( $^{\circ}C$ )  
 $T_{abm, ref}$ : reference temperature of cell ( $^{\circ}C$ )  
 $T_{cell}$ : temperature of cell ( $^{\circ}C$ )  
 $U_L$ : overall heat loss coefficient ( $W/K.m^2$ )  
 $U_t$ : overall top loss coefficient from the cell to the ambient ( $W/K.m^2$ )  
 $U_b$ : back loss coefficient ( $W/K.m^2$ )  
 $V_w$ : wind velocity (m/s)  
 $V$ : voltage at load (V)  
 $V_{oc}$ : open circuit voltage (V)  
 $V_{mp}$ : maximum power point voltage (V)  
 $\gamma_s$ : solar azimuth angle  
 $\rho$ : reflectance  
 $\theta$ : angle of incidence of surface for beam radiation  
 $\theta_c$ : acceptance half angle  
 $\theta_z$ : zenith angle  
 $\epsilon_{bs}$ : emissivity of the back surface  
 $\epsilon_g$ : emissivity of the glass cover  
 $\eta_{el}$ : electrical efficiency of cell  
 $\eta_{el, ref}$ : reference electrical efficiency of cell  
 $\eta_{el, mp}$ : maximum power point electrical efficiency  
 $\sigma$ : Stefan-Boltzmann constant ( $W/m^2.K^4$ )  
 $\tau\alpha$ : product of transmittance absorbance product of solar cell  
 $\tau$ : transmittance of solar cell

## ACKNOWLEDGMENT

The authors are grateful for the financial support and facilities provided by King Fahd University of Petroleum and Minerals.

## REFERENCES

- [1] J. Sun and M. Shi, "Numerical simulation of electric-thermal performance of a solar concentrating photovoltaic/thermal system," in *Proc. 2009 Asia-Pacific Power and Energy Engineering Conference*, Mar. 2009, pp. 1-4.
- [2] T. K. Mallick and P. C. Eames, "Design and fabrication of low concentrating second generation PRIDE concentrator," *Solar Energy Materials and Solar Cells*, vol. 91, no. 7, pp. 597-608, Apr. 2007.
- [3] I. Zanesco and E. Lorenzo, "Optimisation of an asymmetric static concentrator: the PEC-44D," *Progress in Photovoltaics: Research and Applications*, vol. 10, no. 5, pp. 361-376, 2002.
- [4] K. Yoshioka, A. Suzuki, and T. Saitoh, "Performance evaluation of two-dimensional compound elliptic lens concentrators using a yearly distributed insolation model," *Solar Energy Materials and Solar Cells*, vol. 57, no. 1, pp. 9-19, Feb. 1999.
- [5] T. K. Mallick, P. C. Eames, T. J. Hyde, and B. Norton, "The design and experimental characterisation of an asymmetric compound parabolic photovoltaic concentrator for building façade integration in the UK," *Solar Energy*, vol. 77, no. 3, pp. 319-327, Sep. 2004.
- [6] J. Nilsson, H. Håkansson, and B. Karlsson, "Electrical and thermal characterization of a PV-CPC hybrid," *Solar Energy*, vol. 81, no. 7, pp. 917-928, Jul. 2007.
- [7] T. K. Mallick, P. C. Eames, and B. Norton, "Power losses in an asymmetric compound parabolic photovoltaic concentrator," *Solar Energy Materials and Solar Cells*, vol. 91, no. 12, pp. 1137-1146, Jul. 2007.

- [8] M. Brogren, J. Wennerberg, R. Kapper, and B. Karlsson, "Design of concentrating elements with CIS thin-film solar cells for façade integration," *Solar Energy Materials and Solar Cells*, vol. 75, no. 3-4, pp. 567-575, Feb. 2003.
- [9] R. Tang, M. Wu, Y. Yu, and M. Li, "Optical performance of fixed east-west aligned CPCs used in China," *Renewable Energy*, vol. 35, no. 8, pp. 1837-1841, Aug. 2010.
- [10] M. Brogren and P. E. R. Nostell, "Optical efficiency of a pv – thermal hybrid CPC module for high latitudes," *Solar Energy*, vol. 69, no. 1988, pp. 173-185, 2001.
- [11] L. Guiqiang, P. Gang, Y. Su, Z. Xi, and J. Jie, "Preliminary study based on building-integrated compound parabolic concentrators (CPC) PV/thermal technology," *Energy Procedia*, vol. 14, pp. 1, Jan. 2012.
- [12] S. S. Mahammed, T. Ahmed, Y. Hameed, and J. Khalaf, "Theoretical study of the compound parabolic trough solar collector," *Tikrit Journal of Engineering Sciences*, vol. 19, no. 2, pp. 1-10, 2012.
- [13] J. Sun and M. Shi, "Numerical study on optical and electric-thermal performance for solar concentrating PV/T air system," *Science in China Series E: Technological Sciences*, vol. 52, no. 12, pp. 3514-3520, Dec. 2009.
- [14] S. Hatwaambo, "Performance analysis of low concentrating PV-CPC systems with structured reflectors," in *Solar Power*, R. Rugescu, Ed., InTech., 2012, ch. 12.
- [15] S. A. Kalogirou, "Use of TRNSYS for modelling and simulation of a hybrid pv-thermal solar system for Cyprus," *Renewable Energy*, vol. 23, no. 2, pp. 247-260, Jun. 2001.
- [16] J. A. Duffie and W. A. Beckman, *Solar Engineering of Thermal Process*, 3<sup>rd</sup> ed., John Wiley & Sons, Ltd., 2006.
- [17] W. H. McAdams, *Heat Transmission*, 3<sup>rd</sup> ed., McGraw Hill, New York, 1954.



**Haider Ali** was born in Karachi, Pakistan in 1986. He earned his B.E. degree in mechanical engineering from NED University of Engineering and Technology, Pakistan, in 2008. In December 2008, he joined NED University as a lecturer. He completed his master degree of engineering from NED University in 2011. In 2012, he joined King Fahd University of Petroleum and Minerals (KFUPM), where he is currently pursuing his PhD degree in mechanical engineering.

His research interests include thermo-fluids, nanoscale heat transfer, phonon transport and thermodynamics analysis of thermoelectric generator.



**P. Gandhidasan** is a professor of mechanical engineering at King Fahd University of Petroleum and Minerals (KFUPM), Dhahran, Saudi Arabia. He received his PhD degree in mechanical engineering from the Indian Institute of Technology, Madras, in 1979. He has over 34 years of teaching and research experience and has published over 100 technical journal/conference papers.